

Two-stage stochastic approximation for dynamic rebalancing of shared mobility systems

Joseph Warrington* and Dominik Ruchti†

Abstract

Mobility systems featuring shared vehicles are often unable to serve all potential customers, as the distribution of demand does not coincide with the positions of vehicles at any given time. System operators often choose to reposition these shared vehicles (such as bikes, cars, or scooters) actively during the course of the day to improve service rate. They face a complex dynamic optimization problem in which many integer-valued decisions must be made, using real-time state and forecast information, and within the tight computation time constraints inherent to real-time decision-making. We first present a novel nested-flow formulation of the problem, and demonstrate that its linear relaxation is significantly tighter than one from existing literature. We then adapt a two-stage stochastic approximation scheme from the generic SPAR method of Powell *et al.*, in which rebalancing plans are optimized against a value function representing the expected cost (in terms of fulfilled and unfulfilled customer demand) of the future evolution of the system. The true value function is approximated by a separable function of contributions due to the rebalancing actions carried out at each station and each time step of the planning horizon. The new algorithm requires surprisingly few iterations to yield high-quality solutions, and is suited to real-time use as it can be terminated early if required. We provide insight into this good performance by examining the mathematical properties of our new flow formulation, and perform rigorous tests on standardized benchmark networks to explore the effect of system size. We then use data from Philadelphia’s public bike sharing scheme to demonstrate that the approach also yields performance gains for real systems.

1 Introduction

Shared mobility systems, in which vehicles such as bicycles, scooters, and cars are used on demand by customers for a point-to-point journey, are an integral part of many transportation networks. A substantial fraction of cities worldwide have public bike sharing schemes, and at time of writing a recent trend has emerged toward so-called “station free” services featuring bicycles, scooters or cars that can be unlocked via smartphone apps and left in any legal public location after customers complete journeys.

Operators of such schemes, be they city franchise holders or autonomous private companies, typically aim to maximize the number (or total value) of journeys the system is able to support, particularly in cases where

*Simons Institute for the Theory of Computing, UC Berkeley, 121 Calvin Lab, Berkeley, CA 94720-2190, USA; Automatic Control Lab, ETH Zurich, Physikstrasse 3, 8092 Zurich, Switzerland. E-mail: warrington@control.ee.ethz.ch.

†Automatic Control Lab, ETH Zurich, Physikstrasse 3, 8092 Zurich, Switzerland.

customers pay a flat annual fee to access the service. Since customer demand is not evenly distributed over the network, improving the service rate typically requires that paid staff redistribute the shared vehicles manually. Although some of these actions can be planned ahead of time, an online optimization approach, solving what is known as the Dynamic Routing and Repositioning Problem (DRRP), [11], offers operators the ability to respond to the real-time state of the network, thereby mitigating forecast uncertainty and modelling error. Some existing systems allow private agents to participate in the rebalancing effort alongside the operator by offering appropriate incentives [17]. Examples include the Bike Angels program¹ for Citibike in New York City, and the Charger program² offered by Bird.

Existing literature for dynamic shared mobility management, including formulations featuring autonomous vehicles and on-demand ride sharing, falls into two broad categories in terms of theoretical motivation, namely optimization-based and queuing- (or inventory-) theoretic.

Optimization-based methods directly model the system’s costs, constraints, dynamics and demand data, and return an explicit system balancing decision, which may also include pricing decisions. Nair and Miller-Hooks [14] considered the short-term problem of redistributing shared vehicles (SVs) as a chance-constrained integer program, in which demand rates were assumed constant and the operator wishes to serve most demand across rental locations with high probability. Ghosh *et al.* [11] used Lagrangian relaxation (LR) to optimize routing and redeployment actions for a bike-sharing scheme against a pricing function representing the value of bikes at different nodes and different times. They encounter a common trade-off of LR for large-scale problems, between the complexity of solving the decomposed subproblems and the quality of the solution once the algorithm has converged [10]. They cluster the stations in the Boston test system in order to limit the computational complexity of each iteration and obtain a solution with acceptable accuracy; nevertheless the total computation time for a city-scale problem is on the order of a day. Pfrommer *et al.* used deterministic-equivalent forecasts of customer behaviour, and assumptions on their price sensitivity, to construct simultaneous schedules of system rebalancing actions and real-time prices for users [17]. Other recent studies have focused on refining real-time matching algorithms to allocate customers to vehicles at city scale in a ride-sharing context [2, 13].

Recent examples of optimization-based control have employed so-called commodity flow formulations borrowed from the network flow literature [1]. In this setting, customers and shared vehicles are treated as fluid flows along capacitated links, where the links represent roads and vehicles holding a limited number of vehicles or passengers; [23, 25] are two recent examples from literature on routing autonomous vehicles. An attraction of such formulations is that they can either assume away integrality constraints owing to the scale of the problem, or potentially harness long-known results from single- or multi-commodity flow theory when integrality constraints are important.

In contrast, queuing models of mobility systems leverage theory designed for stochastic queuing processes, and are therefore able to design pricing or other control policies accounting for this randomness [3, 22, 24]. Inventory models such as [20] are inspired by mathematically similar problems of this kind from the operations research literature, and lead to a similar search for optimal *policies*, rather than explicit control actions. A drawback to these models, however, is that modelling time-varying input data is significantly harder than

¹<https://www.citibikenyc.com/bikeangels/>, accessed September 2018

²<https://www.bird.co/charger>, accessed September 2018

in a model-based optimization setting, though new preliminary results exist [4].

This paper aims to combine the stochastic modelling strengths of queuing-theoretic approaches with the model-based philosophy of optimization-based approaches. We propose a novel method based on stochastic approximation [5], in which a finitely-parameterized function is used to represent a function from a broader class as accurately as possible (according to a specifically defined metric). This approach is commonplace in reinforcement learning literature, where “optimal” coefficients for a vector of pre-selected basis function are learned from sampled behaviour of the system [8]. In the case of shared mobility, we are interested in estimating the expected value of all customer journeys, under random demand patterns, as a function of the operator’s rebalancing decisions. This value function (VF) allows the operator to optimize its actions against an accurate representation of this expected value (or equivalently, the expected losses from journeys that cannot occur due to poorly positioned SVs), thereby improving the realized service rate in expectation.

One approach to obtaining an accurate VF would be to estimate, for example using Monte Carlo sampling of customer demand scenarios, the expected value of *each state* to which the system operator can drive the system. However, although the search space is enumerable, in that the operator only has to decide where and when (in discretized time) to pick up and deposit a finite number of shared vehicles, the number of possible actions is exponential in the number of stations and time steps. Powell *et al.* suggest approximating the high-dimensional VFs encountered in many operations research problems as a separable sum of functions of their coordinate variables [18]. They describe a stochastic gradient scheme known as *SPAR* to achieve this, and report good performance for two-stage stochastic programs. In other studies such as [19] the same authors applied several related approaches to logistics problems.

In this paper we adapt this scheme to DRRP. We cast the rebalancing problem as a two-stage stochastic program, where the operator makes rebalancing decisions in the first stage without knowledge of the realization of customer demand, which happens in the second stage. The VF of the second stage is approximated as a sum of contributions from rebalancing actions across stations and across time steps, or in other words, as the sum of values of a net change in SVs at a particular place and a particular time. Crucially, the number of parameters needed for this grows only linearly in the number of coordinate variables – number of stations times number of time steps – rather than exponentially. By approximating the second-stage VF in its own right, we separate the difficulties of the first and second stages. The first stage is difficult because it requires the solution of an integer routing and redeployment problem, while the second stage is stochastic in nature. Because the true VF of the second stage is agnostic to the way first-stage decisions are made, an approximation of it can be used a useful intermediate step in generating heuristic or exact solutions to the first-stage problem. In this paper, our approach therefore has two steps, *(i)* approximating the second-stage VF, possibly using a simplified model of the first stage, and *(ii)* re-solving the first-stage problem using the approximate VF as input data in case a full solution was avoided in step *(i)*.

The notion of a separable VF has been used in other shared mobility settings. Raviv *et al.* [20] proved that, if coupling between stations of a bike sharing scheme is ignored, the cost of unsatisfied demand can be written as a convex function of the inventory level. In the *static* rebalancing problem, the operator must arrange the system in an optimal configuration for service rate, but does not intervene after customers start using the system. Separable VFs were studied in [21] for optimizing the overnight “reset” of a bike-sharing scheme before customers start using it in the morning. Pal and Zhang extended the static problem to station-free

bike sharing systems in [15]. The static problem is substantially different from our dynamic setting, because customer actions do not occur simultaneously alongside the operator’s actions. Separable functions were also used in a dynamic, deterministic-equivalent setting in [17] for the problem of offering customer incentives to make modified journeys that are favourable to the system’s service rate. Legros [12] has also computed station VFs and associated Bernoulli policies for dynamic bike sharing, but without explicit predictive modelling of the kind we include here. Brinkmann *et al.* used non-parametric VF estimates, in a similar dynamic look-ahead context to ours, but without considering vehicle routing in the decision problem [7].

1.1 Contributions

Formally, we make the following contributions:

1. We provide a network flow formulation of DRRP whose optimal value is the same as the formulation of [11], but which has a tighter linear relaxation (meaning always at least as tight, and often much tighter);
2. We derive a two-stage approximation scheme adapted from [18] that accommodates stochastic demand and journey values, and uses a separable VF to represent the costs of customer actions as a function of the system operator’s rebalancing actions;
3. We provide insight into the structure of the two-stage formulation, showing that both stages are closely related to network flow problems with integer capacity constraints;
4. We show that this scheme yields highly satisfactory system performance within computation times suitable for real-time implementation. We demonstrate the method using rigorous tests on standardized networks, and a case study using public data from Philadelphia’s public bike sharing scheme.

The paper is structured as follows. Section 2 describes the flow formulation of DRRP, and derives some basic results concerning its decomposition into two stages. Section 3 outlines the iterative value function approximation used to solve the problem. Section 4 presents numerical results for synthetic systems and a model of the Philadelphia network, and Section 5 concludes.

2 Problem statement

In DRRP, the operator must plan routes and load/unload schedules for a fleet \mathcal{V} of operator vehicles over T discrete time steps, in order to maximize the number of successful journeys made by customers during the same forecast horizon.

2.1 Definitions

Let $\mathcal{G}_c := (\mathcal{N}_c, \mathcal{E}_c)$ be a directed graph describing possible customer movements while using a SV, such that movement between from node i to j in \mathcal{N}_c is only possible if $(i, j) \in \mathcal{E}_c$. Let $f_{i,j}^{t,k}$ be the number of customers

wishing to travel from node i to node j at time t , and with journey duration $k \in \{0, \dots, K\}$ time steps for some maximum modelled duration K . We will use the tuple (i, j, t, k) as shorthand.

Let the decision variable $w_{i,j}^{t,k} \in \mathbb{N}$ represent the number of journeys that do take place, and let the loss function $l_{i,j}^{t,k} : \mathbb{N} \rightarrow \mathbb{R}$ represent the social cost of potential journeys that do not occur, such that $l_{i,j}^{t,k}(f_{i,j}^{t,k} - w_{i,j}^{t,k})$ is the cost of unserved demand for tuple (i, j, t, k) . We assume that customer journey values are decoupled within and between such tuples, and that $l_{i,j}^{t,k}$ is defined to penalize journeys in increasing order of their value. Thus, $l_{i,j}^{t,k}(\cdot)$ can be represented as a convex piecewise affine function passing through the origin, evaluated only at integer arguments.

We introduce stochasticity into the model by allowing scalars $f_{i,j}^{t,k}$ and functions $l_{i,j}^{t,k}(\cdot)$ to depend on a random variable ξ sampled from a probability distribution with support Ξ . All other input data to the problem remains deterministic. Thus we have $f_{i,j}^{t,k} : \Xi \rightarrow \mathbb{N}$ and $l_{i,j}^{t,k} : \mathbb{N} \times \Xi \rightarrow \mathbb{R}$. We use $\mathbb{E}[\cdot]$ to denote expectation over ξ . In the remainder of this paper we use the variants $f_{i,j}^{t,k}$, $f_{i,j}^{t,k}(\xi)$, $l_{i,j}^{t,k}(\cdot)$, and $l_{i,j}^{t,k}(\cdot, \xi)$ according to whether or not ξ is relevant to the discourse.

Let $\mathcal{G}_v := (\mathcal{N}_v, \mathcal{E}_v)$ be a directed graph describing possible movements of a set \mathcal{V} of rebalancing vehicles (RVs), such that an RV can move from node i to j in \mathcal{N}_v only if $(i, j) \in \mathcal{E}_v$. Let $z_{v,i,j}^t \in \{0, 1\}$ denote the binary decision variable associated with movement of RV $v \in \mathcal{V}$ from node i to node j at time t , which we assume always takes exactly one time step. The associated cost is denoted $c_{i,j}^{t,k}$.

RVs are used to reposition SVs by loading and unloading them at nodes in \mathcal{N}_c , and travelling with them on board. For the problem to be non-trivial, we must assume that $\mathcal{N}_v \cap \mathcal{N}_c \neq \emptyset$ so that RVs are able to access some of the nodes in \mathcal{N}_c .

Integer variables $y_{v,i}^{+,t}$ and $y_{v,i}^{-,t}$ represent the loading and unloading of SVs onto and from RVs respectively, for $i \in \mathcal{N}_v \cap \mathcal{N}_c$. At time step t , the number of SVs travelling along edge $(i, j) \in \mathcal{E}_v$ inside RVs is denoted $b_{i,j}^t$, and this is bounded by the sum of capacities of the relevant RVs, denoted \bar{b}_v . The number of SVs at node $i \in \mathcal{V}_c$, *after* accounting for any journeys finishing during time step t , is denoted $d_i^t \in \mathbb{Z}$. The SV storage capacity of the node is denoted \bar{d}_i .

2.2 Assumptions

We make the following modelling assumptions:

- (A1) A customer does not enter the system if (a) he cannot start his journey due to a lack of SVs available at his desired starting node, or if (b) doing so would cause the end node to exceed its SV capacity. He does not attempt to start a journey from a different node.
- (A2) Journey times along edges in \mathcal{E}_v and \mathcal{E}_c are deterministic and independent of any of the actions we model, i.e., they are determined entirely by exogenous factors such as signals at junctions and the prevailing level of congestion. They are identical for all RVs, for whom the edges of \mathcal{E}_v always take 1 time step to traverse, but they can differ between SVs, and this is modelled as demand characterized by different values of the lag index k . Travel time parameters for SVs are allowed to vary with the start time t .

(A3) The maximum number of SV journeys starting at node i and time t is bounded by the number present at the end of the previous time step, d_i^{t-1} . In case there are insufficient shared vehicles at a node i and time t for the sum of all demand, i.e. $d_i^{t-1} < \sum_{j,k} f_{i,j}^{t,k}$, the system operator can choose which journeys should take place. This contrasts with the approach of [11], which can be viewed as conservative.³

(A4) RVs are identical with capacity \bar{b} , and we define the variable $z_{i,j}^t := \sum_{v \in \mathcal{V}} z_{v,i,j}^t$ to denote the number of RVs travelling from node i to node j of \mathcal{G}_v at time t .

2.3 Network flow formulation of DRRP

For a given realization $\xi \in \Xi$, the DRRP is presented in problem (1). This can be viewed as a conversion of the DRRP formulation of [11, Table 4] into an equivalent “nested network flow” form, in the sense that the two problems have the same optimal value and optimal solutions can be mapped from one form to the other. The system operator controls flows of RVs $z_{i,j}^t$, flows of SVs $b_{i,j}^t$, and load/unload decisions $y_i^{+,t}$ and $y_i^{-,t}$ at stations, on the assumption that customers then make optimal use of the resulting arrangement to complete their journeys. The flows are nested in the sense that on any edge (i, j) at time t , SVs flows $b_{i,j}^t$ for rebalancing are constrained by the storage capacity of the RVs moving along the same edge, $\bar{b}z_{i,j}^t$.

$$\min_{z, y, b, w, d} \sum_{t=1}^T \left[\sum_{(i,j) \in \mathcal{E}_c} \sum_{k=0}^K l_{i,j}^{t,k} (f_{i,j}^{t,k}(\xi) - w_{i,j}^{t,k}; \xi) + \sum_{(i,j) \in \mathcal{E}_v} c_{i,j}^t z_{i,j}^t + \sum_{i \in \mathcal{N}_c \cap \mathcal{N}_v} r_i^t (y_i^{+,t} + y_i^{-,t}) \right] \quad (1a)$$

$$\text{s. t. } d_i^t = d_i^{t-1} + \sum_{k=0}^K \left(\sum_{(j,i) \in \mathcal{E}_c} w_{j,i}^{t-k,k} - \sum_{(i,j) \in \mathcal{E}_c} w_{i,j}^{t,k} \right) + y_i^{-,t} - y_i^{+,t}, \quad t = 1, \dots, T, \quad i \in \mathcal{N}_c, \quad (1b)$$

$$\sum_{(i,j) \in \mathcal{E}_v} b_{i,j}^t = \sum_{(j,i) \in \mathcal{E}_v} b_{j,i}^{t-1} + y_i^{+,t} - y_i^{-,t}, \quad t = 1, \dots, T, \quad i \in \mathcal{N}_v, \quad (1c)$$

$$\sum_{(i,j) \in \mathcal{E}_v} z_{i,j}^t = \sum_{(j,i) \in \mathcal{E}_v} z_{j,i}^{t-1}, \quad t = 1, \dots, T, \quad i \in \mathcal{N}_v, \quad (1d)$$

$$0 \leq b_{i,j}^t \leq \bar{b}z_{i,j}^t, \quad t = 0, \dots, T \text{ and } b_{i,j}^0 \in \mathbb{Z} \text{ given,} \quad (1e)$$

$$0 \leq w_{i,j}^{t,k} \leq f_{i,j}^{t,k}(\xi), \quad t = 1, \dots, T, \text{ and } w_{i,j}^{t,k} \text{ given for } 1 - K \leq t \leq 0, \quad -t < k \leq K, \quad (1f)$$

$$0 \leq d_i^t \leq \bar{d}_i, \quad t = 0, \dots, T \text{ and } d_i^0 \in \mathbb{Z} \text{ given,} \quad (1g)$$

$$0 \leq y_i^{+,t} \leq \bar{y}, \quad 0 \leq y_i^{-,t} \leq \bar{y}, \quad t = 1, \dots, T, \quad i \in \mathcal{N}_c, \quad (1h)$$

$$z_{i,j}^0 \text{ given such that } \sum_{i,j} z_{i,j}^0 = |\mathcal{V}|, \quad (1i)$$

$$w_{i,j}^{t,k} \in \mathbb{Z} \text{ for all tuples } (i, j, t, k). \quad (1j)$$

$$y_i^{+,t}, y_i^{-,t}, b_{i,j}^t \in \mathbb{Z} \text{ for all indices.} \quad (1k)$$

$$z_{i,j}^t \in \mathbb{Z}, \quad t = 1, \dots, T, \quad (i, j) \in \mathcal{E}_v, \quad (1l)$$

Constraint (1b) enforces conservation of SVs at each customer node i and time t . The model allows for SVs to “jump” from station i to j during a time step, modelling very short journeys as duration $k = 0$ discrete

³Ghosh *et al.* [11] impose an additional “fair sharing” constraint meaning that, in our notation, integer valued $w_{i,j}^{t,k}$ are no greater than their demand share of the d_i^{t-1} available SVs. Thus, if for some (i, t, k) there are 9 SVs present, and 10 destinations j for which $f_{i,j}^{t,k} = 1$, no journeys can occur at all, because one must enforce $w_{i,j}^{t,k} \leq \frac{9}{10}$ for each destination j .

steps.

Constraint (1c) enforces the conservation of SVs at the nodes of \mathcal{G}_v , i.e., while the SVs are loaded inside RVs. Constraint (1d) enforces conservation of the RVs themselves, and (1e) bounds the number of SVs travelling along an edge in \mathcal{E}_v by the summed capacities of RVs travelling along the same edge, which are equal under Assumption A3.

Constraint (1f) bounds the number of journeys by the level of demand present for each tuple (i, j, t, k) . As our formulation is intended for a real-time implementation, we allow some journeys already to be in progress at time 0, with this having implications on constraint (1b). Constraint (1g) bounds the number of SVs that can be accommodated at each node $i \in \mathcal{N}_c$, and specifies the initial “fill level” at each node. Constraint (1h) limits loading and unloading actions to be nonnegative, and upper-bounds them by some constant $\bar{y} \leq \bar{b}|\mathcal{V}|$ representing the largest single rebalancing action contemplated by the operator. Note that constraints (1e) and (1f) together ensure that $y_i^{+,t}$ and $y_i^{-,t}$ are zero unless $z_{i,j}^t = 1$ for some j satisfying $(i, j) \in \mathcal{E}_v$, i.e., a RV is passing through at the right place at the right time.

Constraint (1i) specifies that RV flows must correspond to integer-valued numbers of RVs, with initial conditions corresponding to the number of RVs $|\mathcal{V}|$ present. Constraints (1l) and (1k) specify that SV transport flows, RV movement decisions, SV loading/unloading actions, and customer journeys are all integer-valued.

For brevity we use symbols z, y, b, w, d to refer to concatenations of their corresponding indexed quantities.

Remark 1. *In addition to the social cost of unserved demand, $\sum_{i,j,t,k} l_{i,j}^{t,k}(w_{i,j}^{t,k})$, one may also be interested in the service rate, defined as the ratio of completed journeys to total demand, $\sum_{i,j,t,k} w_{i,j}^{t,k} / \sum_{i,j,t,k} f_{i,j}^{t,k}$. This metric has the convenience of being invariant to system size. The service rate can be accommodated as an objective function by setting $l_{i,j}^{t,k}(x; \xi) = x$ and all other costs to zero. The objective function to minimize, when normalized by $\sum_{i,j,t,k} f_{i,j}^{t,k}(\xi)$, will then be equal to 1 minus the service rate.*

2.3.1 Strength of relaxation

Numerical tests show the relaxation of (1) to be at least as tight, and very often much tighter, than the linear program (LP) relaxation of the mixed-integer formulation presented in [11, Table 4]). This is because (1) models the conservation of SVs being transported by RVs more explicitly. The full MIP can also be solved considerably faster on average. We tested the strength of the relaxation on deterministic benchmark instances of a bike-sharing problem, which were created via the same procedure and parameters described in Section 4.2, and solved on the same hardware, as for the main numerical results of this paper. For a fair comparison with [11], all loss functions were modelled as deterministic linear functions $l_{i,j}^{t,k}(x) = x$, and the “fair sharing” constraint [11, eq. (3)] was not enforced.⁴

Table 1 shows average results over 10 instances for each row, using the standardized test networks described in Section 4.2. Problems were solved in Gurobi to within a relative tolerance of 10^{-3} , and a time limit of 600 seconds was enforced. The *LP gap* columns report the average percentage decrease in solver objective

⁴Qualitatively similar results were obtained when this constraint was added to both models, but we omit these for brevity.

Table 1: Comparison of LP relaxation strengths of formulations (1) and [11, Table 4].

$ \mathcal{N}_c $	$ \mathcal{V} $	Rel. LP gap (%)		Solution time (seconds)				Average demand	Service rate (%)		
		(1)	[11]	(1) LP	(1)	[11] LP	[11]		No action	(1)	
4	1	26.8	26.8	0.003	0.02	0.002	0.01	31.4	93.2	98.9	
9	1	25.7	34.9	0.015	0.32	0.007	0.36	76.2	85.9	98.1	
	3	8.5	21.5	0.016	0.28	0.016	21.11				99.5
16	1	51.4	58.8	0.060	3.44	0.024	2.23	151.8	84.3	93.8	
	3	3.8	10.3	0.054	88.76	0.058	249.06				98.3
25	1	30.7	57.4	0.135	10.61	0.072	15.09	232.2	80.9	88.4	
	3	27.4	29.9	0.138	194.64	0.119	356.16				95.4
	5	15.1	18.0	0.144	213.47	0.205	493.22				97.8
36	1	19.2	39.6	0.233	12.86	0.126	7.60	321.5	81.5	86.9	
	3	35.8	49.0	0.298	382.59	0.247	398.18				93.7
	5	24.1	32.0	0.292	182.90	0.388	531.38				96.6
	7	7.6	20.8	0.290	154.87	0.581	528.69				97.1

when integrality constraints were relaxed, relative to the best solution of (1) found in the time limit. In the *Solution time* columns, the *LP* columns indicate time for the relaxations, and the others indicate MIP solve times. We mark cases where at least one problem instance timed out with an asterisk. The final two columns indicate respectively the average service rates with no operator intervention and with interventions returned by solving (1) until timeout or an optimal solution was found. Test results are shown for sizes of system that could be solved directly as an MIP across multiple instances within a reasonable time.

2.4 Model scope

Formulation (1) can be used to model a number of different shared mobility scenarios:

1. Conventional bike sharing services, in which indices i and j represent docking stations, vehicles v represent trucks able to carry up to \bar{b}_v bikes between docking stations, and the finite capacity of each station i is represented by \bar{d}_i .
2. Station-free shared bike services such as LimeBike, Mobike, and Ofo, in which the number of “notional stations” $|\mathcal{N}_c|$ tends to infinity as space is divided into increasingly fine partitions. Since such bikes can be left freely in public spaces, the capacity of the notional stations can be considered unbounded by setting $\bar{d}_i = +\infty$.
3. Shared e-scooter services such as eCooltra and Bird. In the case of “micro” scooters, these distinguish themselves from bikes in that, owing to their small size, large numbers can in principle be repositioned by a single manned vehicle, i.e., $\bar{b}_v = +\infty$.
4. Point-to-point car sharing services such as Zipcar Flex and Car2Go, in which only one vehicle can be transported at a time by a single staff member. In this setting, $z_{i,j}^t$ corresponds to the movements of *staff*, rather than trucks that can contain shared vehicles.

2.5 Two-stage stochastic program

The operator wishes to solve (1) to minimize expected costs over all possible realizations of ξ . We consider a setting in which the operator chooses decisions z and y before observing ξ , and carries out its decision in full during the planning horizon. In stochastic programming terminology, the decision-maker optimizes without recourse.⁵ This can be cast as a two-stage stochastic program. The first stage is

$$\min_{z,y,b} \sum_{t=1}^T \left[\sum_{(i,j) \in \mathcal{E}_v} c_{i,j}^t z_{i,j}^t + \sum_{i \in \mathcal{N}_c \cap \mathcal{N}_v} r_i^t (y_i^{+,t} + y_i^{-,t}) \right] + \mathbb{E}[V(y, \xi)] \quad (2a)$$

$$\text{s. t.} \quad \sum_{(i,j) \in \mathcal{E}_v} b_{i,j}^t = \sum_{(j,i) \in \mathcal{E}_v} b_{j,i}^{t-1} + y_i^{+,t} - y_i^{-,t}, \quad t = 1, \dots, T, \quad i \in \mathcal{N}_v, \quad (2b)$$

$$\sum_{(i,j) \in \mathcal{E}_v} z_{i,j}^t = \sum_{(j,i) \in \mathcal{E}_v} z_{j,i}^{t-1}, \quad t = 1, \dots, T, \quad i \in \mathcal{N}_v, \quad (2c)$$

$$0 \leq b_{i,j}^t \leq \bar{b} z_{i,j}^t, \quad t = 0, \dots, T \text{ and } b_{i,j}^0 \in \mathbb{Z} \text{ given,} \quad (2d)$$

$$0 \leq y_i^{+,t} \leq \bar{y}, \quad 0 \leq y_i^{-,t} \leq \bar{y}, \quad t = 1, \dots, T, \quad i \in \mathcal{N}_c, \quad (2e)$$

$$z_{i,j}^0 \in \mathbb{Z} \text{ given such that } \sum_{i,j} z_{i,j}^0 = |\mathcal{V}|, \quad (2f)$$

$$y_i^{+,t}, y_i^{-,t}, b_{i,j}^t \in \mathbb{Z} \text{ for all indices.} \quad (2g)$$

$$z_{i,j}^t \in \mathbb{Z}, \quad t = 1, \dots, T, \quad (i, j) \in \mathcal{E}_v, \quad (2h)$$

in which $V(y, \xi)$ represents the second-stage cost resulting from rebalancing actions y , for demand realization ξ . The second-stage problem is

$$V(y, \xi) := \min_w \sum_{t=1}^T \left[\sum_{(i,j) \in \mathcal{E}_c} \sum_{k=0}^K l_{i,j}^{t,k} (f_{i,j}^{t,k}(\xi) - w_{i,j}^{t,k}; \xi) \right] \quad (3a)$$

$$\text{s. t.} \quad 0 \leq d_i^0 + \sum_{\tau=1}^t \left[\sum_{k=0}^K \left(\sum_{(j,i) \in \mathcal{E}_c} w_{j,i}^{\tau-k,k} - \sum_{(i,j) \in \mathcal{E}_c} w_{i,j}^{\tau,k} \right) + y_i^{-,\tau} - y_i^{+,\tau} \right] \leq \bar{d}_i, \quad t = 1, \dots, T, \quad i \in \mathcal{N}_c, \quad (3b)$$

$$0 \leq w_{i,j}^{t,k} \leq f_{i,j}^{t,k}(\xi), \quad t = 1, \dots, T, \quad \text{and } w_{i,j}^{t,k} \text{ given for } 1 - K \leq t \leq 0, \quad -t < k \leq K, \quad (3c)$$

$$w_{i,j}^{t,k} \in \mathbb{Z} \text{ for all tuples } (i, j, t, k). \quad (3d)$$

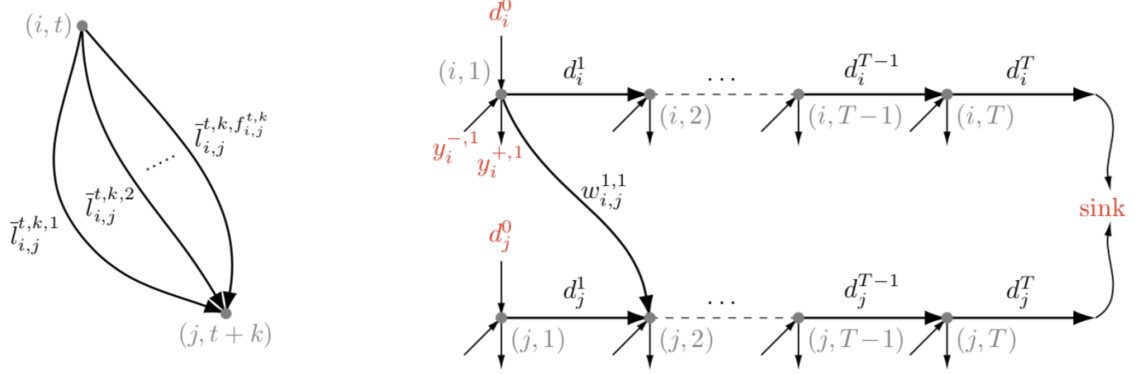
Constraint (3b) combines (1c) and (1g). This eliminates the station fill level variables d_i^t , which are used in (1) only for exposition, by writing $d_i^t = d_i^0 + \sum_{\tau=1}^t \left[\sum_{k=0}^K \left(\sum_{(j,i) \in \mathcal{E}_c} w_{j,i}^{\tau-k,k} - \sum_{(i,j) \in \mathcal{E}_c} w_{i,j}^{\tau,k} \right) + y_i^{-,\tau} - y_i^{+,\tau} \right]$.

2.6 Properties of the second stage

We now prove two important properties of the second stage, and discuss the feasibility of problem (3).

Proposition 1 (Tight LP relaxation). *If the constraints of problem (3) have integer-valued right-hand sides, the problem has an integer-valued solution even when when integrality constraint (3d) is relaxed.*

⁵Of course, in practice such adaptation can still be carried out by computing new (z, y) schedules partway through the horizon in light of the new system state and forecast inputs. In our formulation the ‘‘here-and-now’’ decisions do not account for this additional possibility.



(a) Model of flow $w_{i,j}^{t,k}$ as the sum of flows along unit-capacity edges, whose costs $\bar{l}_{i,j}^{t,k,\cdot}$ are negated slopes of the piecewise linear cost function $l_{i,j}^{t,k}(f_{i,j}^{t,k}(\xi) - w_{i,j}^{t,k}, \xi)$. Optimal flow solutions are equivalent to objective (3a) when the constant $l_{i,j}^{t,k}(f_{i,j}^{t,k}(\xi); \xi)$ is added.

(b) Schematic of second stage as a min-cost flow problem. For clarity only two station rows i, j and one SV flow $w_{i,j}^{1,1}$ are shown. Each flow $w_{i,j}^{t,k}$ is modelled as illustrated in panel (a). The sink value is equal to the sum of net supply elsewhere in the system. Nodes and their labels are depicted in grey. Each horizontal edge has cost zero and capacity \bar{d}_i or \bar{d}_j .

Figure 1: Model of the second stage (3) as a min-cost flow problem.

Proof. We show that the optimization over w can be written as a min-cost flow problem [1, §5] over a directed graph with integer-valued sources, sinks, and edge capacities. It is widely known [19, §5.5] that this guarantees the existence of an integer-valued LP solution.

We first note that since $l_{i,j}^{t,k}(\cdot, \xi)$ is convex and piecewise linear, with breakpoints at every integer argument $\{1, \dots, f_{i,j}^{t,k}(\xi)\}$, it can be represented by the cost of the flow shown in Fig. 1a, in which each edge supports a unit of demand, with cost equal to the negated gradient of the relevant segment of $l_{i,j}^{t,k}(\cdot, \xi)$. In any optimal solution to the flow problem, the edges with the most negative cost, corresponding to the most valuable journeys and the steepest segments of $l_{i,j}^{t,k}(\cdot, \xi)$, will be used first. More precisely, the edge flows model $l_{i,j}^{t,k}(f_{i,j}^{t,k}(\xi) - w_{i,j}^{t,k}, \xi) - l_{i,j}^{t,k}(f_{i,j}^{t,k}(\xi), \xi)$, the latter term being the cost of leaving all customers unserved.

Second, the fill levels of stations can be represented as shown in Fig. 1b. The flow on each horizontal link equals d_i^t and is constrained to the interval $[0, \bar{d}_i]$. At each time step it receives contributions from arriving and departing SVs, each modelled according to the preceding paragraphs, and is subject to load/unload actions $y_i^{+,t}$ and $y_i^{-,t}$. To avoid overcrowding only $y_i^{+,1}$ and $y_i^{-,1}$ are labelled.

SV flows already in progress, $w_{i,j}^{t,k}$ for $1 - K \leq t \leq 0$, whose values are fixed data, are modelled as fixed supply nodes connected to the relevant receiving node of Fig. 1b. SV flows for which $t + k > T$ are modelled as in Fig. 1a, but their end nodes are connected to the sink. To avoid overcomplication, neither of these two types of flow are shown in Fig. 1b.

Lastly, the flows exiting each station row are routed to a common sink with demand set to conserve SVs in the system. Thus the problem can be written in canonical form $\min_x c^\top x$ subject to $\sum_{m \rightarrow n} x_m - \sum_{n \rightarrow p} x_p = b_n \forall n$ and $0 \leq x_l \leq \bar{x}_l \forall l$, where b_n and \bar{x}_l are all integer valued. \square

Remark 2. Problem (3) can be solved using a dedicated min-cost flow solver, which can be significantly

more efficient than a solver designed for generic LPs. This solver must be capable of returning the Lagrange multipliers required by Algorithm 10. Another way of obtaining these multipliers would be to solve the corresponding dual problem [1, eq. (5.2)].

Proposition 2 (Convex value function). *The second-stage VF, $\mathbb{E}[V(y, \xi)]$, is a convex function of y .*

Proof. By introducing epigraph variables to model the piecewise linear functions $l_{i,j}^{t,k}(\cdot, \xi)$, problem (3) can be written in the form

$$V(y, \xi) = \min_x c(\xi)^\top x + d \quad \text{s. t. } Ax \leq b(\xi) + Dy.$$

Thanks to Proposition 1 the integrality constraints are not required. For fixed ξ this satisfies the convexity conditions of [9, Prop. 2.1], where the parameter domain S used in that result corresponds to the projection of the feasible set of (2) onto y -space in our setting. Thus $V(y, \xi)$ is convex in y . The expectation over ξ is simply the linear combination $\mathbb{E}[V(y, \xi)] = \sum_{\xi' \in \Xi} [\mathbb{P}(\xi = \xi') \cdot V(y, \xi')]$, and thus also convex. \square

2.6.1 Feasibility

Problem (3) may not be feasible, depending on the boundary conditions $y_i^{+,t}, y_i^{-,t}$ inherited from the first stage. As a trivial example, consider a system with zero demand ($f_{i,j}^{t,k} = 0$ for all (i, j, t, k)), in which one station i has an initial fill level satisfying $0 \leq d_i^0 \leq \bar{d}_i$ and immediately receives $y_i^{+,1} > \bar{d}_i - d_i^0$ SVs in the first time step, with $y_i^{-,t} = 0$. With all $w_{i,j}^{t,k}$ constrained to zero, constraint (3b) cannot be satisfied.

In reality, the problem of a full end station would be overcome by customers diverting to another station on arrival, and empty initial stations may lead to the customer using a nearby station instead. Thus true infeasibility is never encountered in the real world. Modelling these effects accurately, however, although in principle possible, would introduce substantial extra complexity in the form of additional decision variables and constraints.

We use a modelling simplification to ensure solutions respect (3b) whenever possible. We introduce two extra penalty variables per node i and time step t , which allows SVs to be created or destroyed at a high cost. Thus for each tuple (i, t) constraint (3b) becomes

$$0 \leq d_i^0 + \sum_{\tau=1}^t \left[\sum_{k=0}^K \left(\sum_{(j,i) \in \mathcal{E}_c} w_{j,i}^{\tau-k,k} - \sum_{(i,j) \in \mathcal{E}_c} w_{i,j}^{\tau,k} \right) + y_i^{-,\tau} - y_i^{+,\tau} \right] + p_i^{+,t} - p_i^{-,t} \leq \bar{d}_i,$$

where $p_i^{+,t} \geq 0$ and $p_i^{-,t} \geq 0$ have suitably high linear cost coefficients in the objective. It is straightforward to show that Proposition 1 still holds in this setting, by modifying the graph in Fig. 1b to include an additional source and sink, high-cost edges to and from each node, and zero-cost edges allowing these to be bypassed if the problem is already feasible.

3 Solution approach

In the common case that the number of possible demand realizations is very large or infinite, problem (2)-(3) cannot be solved directly, as this would require an analytical representation of $\mathbb{E}_\xi[V(y, \xi)]$, which is generally

unavailable. The number of possible realizations of ξ could be modelled as exponential in the number of customer nodes where demand arises, $\mathcal{O}(\bar{f}^{|\mathcal{N}_c|})$ where \bar{f} is the number of different integer demand levels per station. Alternatively it could be infinite, for example in the case of a pure Poisson arrival process with no theoretical upper bound on demand per time interval.

One potential compromise is to write a problem resembling (1), but which simultaneously encodes a limited number of realizations $(\xi_{(1)}, \xi_{(2)}, \dots)$ sampled from Ξ , and includes duplicate decision variables $(w_{(1)}, w_{(2)}, \dots)$ and duplicates of constraints (3b)-(3d) for each. The second-stage cost would be represented by the sample average of objective (3a). However, the resulting scenario program has a very large number of decision variables and the number of constraints scales with the number of scenarios; a solution by branch-and-bound is impractical even for small networks.

Another possibility would be to use a decomposition scheme such as LR to break the problem into separable subproblems linked by pricing functions. Such an approach was tried in [11], and while it was possible to use additional clustering heuristics to solve large-scale problems, computation times remained long (significant fractions of a day), even in a deterministic demand setting.

3.1 Separable value function approximation

As an alternative to the approaches discussed above, we propose to solve (2)-(3) using an approximate representation of the second-stage value function,

$$\bar{V}(y; \theta) \approx \mathbb{E}[V(y, \xi)]$$

taking the form

$$\bar{V}(y; \theta) = \theta_0 + \sum_{t=1}^T \sum_{i \in \mathcal{N}_c \cap \mathcal{N}_v} \bar{V}_i^t(y_i^{-,t} - y_i^{+,t}; \theta_i^t), \quad (4)$$

in which $\theta := (\theta_0, \theta_1^1, \dots, \theta_{|\mathcal{N}_v|}^T)$ is a vector of parameters, with $\theta_0 \in \mathbb{R}$ and $\theta_i^t \in \mathbb{R}^{2\bar{y}}$ for each index (i, t) .

Expressing the elements of each station's subvector as $\theta_i^t = ([\theta_i^t]_{-\bar{y}}, [\theta_i^t]_{-\bar{y}+1}, \dots, [\theta_i^t]_{\bar{y}-1})$, each function $\bar{V}_i^t : [-\bar{y}, \bar{y}] \rightarrow \mathbb{R}$ is of the form

$$\bar{V}_i^t(x; \theta_i^t) = \begin{cases} -\sum_{y'=-\bar{y}}^{-1} [\theta_i^t]_{y'}, & x = -\bar{y}, \\ -\sum_{y'=\lceil x \rceil - 1}^{-1} [\theta_i^t]_{y'} + [\theta_i^t]_{\lceil x \rceil - 1} (x - \lceil x \rceil), & -\bar{y} < x < 0, \\ 0, & x = 0, \\ \sum_{y'=0}^{\lfloor x \rfloor} [\theta_i^t]_{y'} + [\theta_i^t]_{\lfloor x \rfloor} (x - \lfloor x \rfloor), & 0 < x < \bar{y}, \\ \sum_{y'=0}^{\bar{y}-1} [\theta_i^t]_{y'}, & x = \bar{y}. \end{cases} \quad (5)$$

Thus, \bar{V}_i^t is a piecewise linear function passing through the origin, and with the $2\bar{y}$ elements of θ_i^t specifying the slopes between its integer breakpoints. We recall that constant \bar{y} is the largest magnitude of action $y_i^{+,t}$ or $y_i^{-,t}$ under consideration by the operator.

In light of Proposition 2, we impose the additional restrictions on θ_i^t that the slopes be non-decreasing (i.e., forming a convex function), and bounded in magnitude by some θ^{\max} ; see Fig. 2. We write the set of feasible

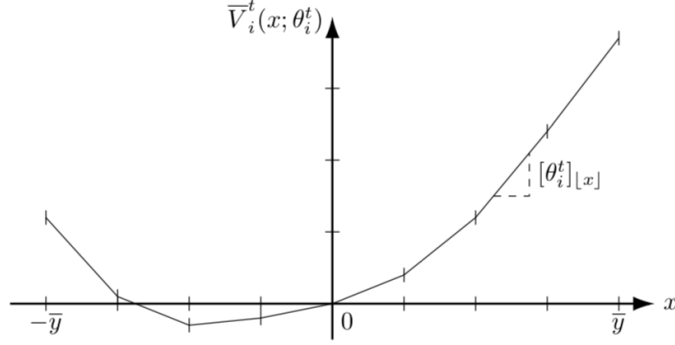


Figure 2: Illustration of the convex value function component $\bar{V}_i^t(\cdot; \theta_i^t)$ defined in equation (5). The elements of the vector θ_i^t specify the $2\bar{y}$ slopes between integer breakpoints, and the function always passes through the origin.

parameters compactly as

$$\Theta := \left\{ \theta \mid \begin{array}{ll} -\theta^{\max} \leq [\theta_i^t]_{y'} \leq \theta^{\max} & y' = -\bar{y}, \dots, \bar{y} - 1, \quad \forall(i, t), \\ [\theta_i^t]_{y'} \geq [\theta_i^t]_{y'-1} & y' = -\bar{y} + 1, \dots, \bar{y} - 1, \quad \forall(i, t) \end{array} \right\}. \quad (6)$$

Problem (2) can now be solved approximately by substituting \bar{V} into the objective in place of $\mathbb{E}_\xi[V(y, \xi)]$:

$$\begin{aligned} \min_{z, y} \quad & \sum_{t=1}^T \left[\sum_{(i,j) \in \mathcal{E}_v} c_{i,j}^t z_{i,j}^t + \sum_{i \in \mathcal{N}_c \cap \mathcal{N}_v} r_i^t (y_i^{+,t} + y_i^{-,t}) \right] + \bar{V}(y; \theta) \\ \text{s. t.} \quad & (2b)-(2h) \end{aligned} \quad (7)$$

We note immediately that since θ_0 appears as a constant offset in the objective of (7), it plays no role in the resulting first-stage decisions. We therefore estimate only the elements θ_i^t , and note that an estimate of θ_0 would be straightforward to obtain with a minor adaptation of the algorithm similar to [18, §3].

3.2 Stochastic approximation algorithm

We now describe an iterative procedure based on the so-called SPAR (*separable, projective, approximation routine*) [18] to estimate the parameterization $\theta^* \in \Theta$, approximating the true expected value of (3), that yields the most efficient solution to the two-stage problem (2)-(3). The procedure is listed in Algorithm 1.

The superscript (n) indicates a variable's value at iteration n . At each iteration, the algorithm uses the result of a sample instance of the second-stage problem (3) to modify the gradient of $\bar{V}(y)$ at the last value of y chosen in the first stage. The modification is determined by the sensitivity of the optimal value of (3) to the first-stage decisions, which is readily obtained via the optimal dual variables for constraints (3b).

The gradient vector ζ in line 11 has the same dimension as θ . Using $[\zeta_i^t]_{y'}$ to denote the element of ζ corresponding to $[\theta_i^t]_{y'}$, it is defined by

$$[\zeta_i^t]_{y'} = \begin{cases} \lambda_i^{+,t} - \lambda_i^{-,t} & \text{if } y' = y_i^{(n)-,t} - y_i^{(n)+,t}, \\ 0 & \text{otherwise,} \end{cases} \quad (8)$$

Algorithm 1 SPAR for dynamic rebalancing of shared mobility systems

Input: $T, \Xi, (\mathcal{V}_v, \mathcal{E}_v), (\mathcal{V}_c, \mathcal{E}_c), n_{\max}$; mappings $f_{i,j}^{t,k}(\xi), l_{i,j}^{t,k}(\cdot, \xi), \alpha(n)$

Output: First-stage actions $(z^{(n_{\max})}, y^{(n_{\max})})$, final parameter vector $\theta^{(n_{\max})}$

Indices: Iteration n , time step t , edges $(i, j) \in \mathcal{E}_c$, durations k

- 1: $\theta^{(1)} \leftarrow \mathbf{0}$
 - 2: **for** $n = 1, \dots, n_{\max}$ **do**
 - 3: Update cost function of (7) with approx. cost-to-go $\bar{V}(y; \theta^{(n)})$
 - 4: $(z^{(n)}, y^{(n)}) \leftarrow$ Solve (7)
 - 5: Draw a new independent sample $\xi^{(n)} \sim \Xi$
 - 6: **for** each tuple (i, j, t, k) **do**
 - 7: Update demand $f_{i,j}^{t,k}(\xi^{(n)})$
 - 8: Update journey valuation function $l_{i,j}^{t,k}(\cdot; \xi^{(n)})$
 - 9: Update RHS of problem (3) with data $y^{(n)}$
 - 10: $\lambda^{(n)} \leftarrow$ Solve convex relaxation of (3) ▷ Multipliers for constraints (3b)
 - 11: Construct gradient vector $\zeta(\lambda^{(n)})$
 - 12: $\tilde{\theta} \leftarrow \theta^{(n)} - \alpha(n)\zeta(\lambda^{(n)})$ ▷ Gradient step
 - 13: $\theta^{(n+1)} \leftarrow \arg \min_{\theta \in \Theta} \frac{1}{2} \|\theta - \tilde{\theta}\|^2$ ▷ Project onto admissible param. set
-

where $\lambda_i^{+,t}$ and $\lambda_i^{-,t}$ are optimal dual variables for the upper and lower bounds of constraint (3b) respectively, and $y_i^{(n),+,t}$ and $y_i^{(n),-,t}$ are outputs from stage 1. The step size $\alpha(n)$ diminishes over iterations, and the asymptotic convergence results derived in [18] rely on this rule satisfying $\alpha(n) \in (0, 1]$, $\sum_{n=1}^{\infty} \alpha(n) = \infty$, and $\sum_{n=1}^{\infty} (\alpha(n))^2 < \infty$.⁶

3.3 Use of continuous relaxations

Thanks to the integer breakpoints in our parameterized approximator $\bar{V}(y; \theta)$, we can guarantee that integer-valued RV routing decisions z result in an integer-valued solution to the whole problem, even when the integrality constraints on y and b are not enforced. This may help to explain the relatively low computation times reported in Section 4. We prove this in the following Lemma and Proposition.

Lemma 3.1. *There always exists an optimizer of (7) with y variables taking the form $(y_i^{+,t}, 0)$ or $(0, y_i^{-,t})$ for all tuples (i, t) .*

Proof. By inspecting the constraints and recalling that the cost coefficients satisfy $r_i^t \geq 0$, it is immediate that for any elements $(y_i^{+,t}, y_i^{-,t})$ of a feasible solution to (7), the modification $(y_i^{+,t} - \min\{y_i^{+,t}, y_i^{-,t}\}, y_i^{-,t} - \min\{y_i^{+,t}, y_i^{-,t}\})$ is feasible and has no greater cost. The result follows. \square

Proposition 3. *If (7) remains feasible when z is fixed to some integer-valued z^* , then this fixed problem has an integer-valued optimal b^* and y^* , even when integrality constraint (2g) is relaxed.*

Proof. With $z = z^*$ fixed, the optimization over the remaining variables can be written as a min-cost network

⁶The original formulation also allows for random step sizes, with slightly different requirements on these for convergence.

a segment’s gradient $[\theta_i^t]_{y'}$ can be obtained, then as long as the probability of visiting each segment has a strictly positive lower bound in the limit, the estimate converges to the true value function almost surely.

Second, the case of choosing the visited segments of a multi-dimensional but separable function as a result of an outer problem was considered. This violates the strictly-positive probability condition described above, because the optimizer will typically visit only a few segments infinitely often. But under a technical stability condition it can be shown [18, Thm. 3] that an accumulation point of the algorithm solves the outer problem in which the value function appears.

Lastly, the authors turn to the case corresponding most closely to our formulation, where a non-separable value function is represented by a sum of separate functions of its coordinate variables. Although the above convergence results no longer apply, they report on a non-separable two-stage stochastic program for which SPAR still produces high-quality solutions. This agrees with our experience.

4 Numerical simulations

We now evaluate the performance of the two-stage approach. In Section 4.1 we describe the treatment of uncertainty in the model, then test our approximation scheme on two sets of test networks. Networks in the first set, described in Section 4.2, are artificially constructed on square grids with dimensionless distance and time units. Customer demand for SVs is clustered such that the system enjoys only a moderate service rate unless rebalancing interventions are made by RVs. We report results on these networks in Section 4.3. Then in Section 4.4 we move on to a case study constructed from public data for Philadelphia’s public scheme.

4.1 Uncertainty model

In all our numerical experiments we model the random arrival of customers wishing to start journeys with an SV as independent events for start-end pairs $(i, j) \in \mathcal{E}_c$, journey durations k , and time steps t . The values of these potential journeys are also considered independent. Thus, the functions $f_{i,j}^{t,k}(\xi)$ and $l_{i,j}^{t,k}(\cdot, \xi)$ could be viewed as independent mappings $f_{i,j}^{t,k}(\xi_{i,j}^{t,k})$ and $l_{i,j}^{t,k}(\cdot, \xi_{i,j}^{t,k})$ from uncorrelated sub-vectors of ξ .

In these experiments we make the standard assumption that events where customers arrive and attempt to start a journey are exponentially distributed in continuous time with known rate parameter. Thus each $f_{i,j}^{t,k}(\xi_{i,j}^{t,k}) \in \mathbb{N}$ follows a separately-parameterized Poisson distribution for each tuple (i, j, t, k) in our discrete time setting. We assume each sampled sub-vector $\xi_{i,j}^{t,k}$ both

- 1) determines the demand level $f_{i,j}^{t,k}(\xi_{i,j}^{t,k})$, and
- 2) parameterizes the associated loss function $l_{i,j}^{t,k}(\cdot, \xi_{i,j}^{t,k})$.

The latter uses $f_{i,j}^{t,k}(\xi_{i,j}^{t,k})$ samples from a uniform distribution $U(l_{\min}, l_{\max})$, with $0 \leq l_{\min} \leq l_{\max}$, sorting the values in ascending order to obtain the convex, piecewise affine loss function described in Section 2.1.⁷

⁷Although conceptually in Algorithm 1 the dimension of ξ should be fixed *a priori*, each loss function $l_{i,j}^{t,k}(\cdot, \xi_{i,j}^{t,k})$ has a random domain $\{0, \dots, f_{i,j}^{t,k}(\xi_{i,j}^{t,k})\}$, and is therefore described by a random number of slope parameters. In practice, one can simply sample the required number of slopes of this function once $f_{i,j}^{t,k}$ has been realized, and view these samples as the first of an arbitrarily long sequence within $\xi_{i,j}^{t,k}$, whose length would be invariant to the realized value $f_{i,j}^{t,k}(\xi_{i,j}^{t,k})$.

Algorithm 2 Creation of artificial scenarios for clustered nominal demand on a rectangular grid

Input: Number of origin and destination clusters (O, D) , time horizon T , SV speed v , step duration Δt

Output: Nominal customer demand $F_{i,j}^{t,k}$ for $(i, j) \in \mathcal{E}_c$, $t = 1, \dots, T$, $k = 0, \dots, K$

Indices:

```

1:  $\mathcal{O} = \emptyset$ ,  $\mathcal{D} = \emptyset$ ,  $F_{i,j}^{t,k} = 0$  for all tuples  $(i, j, t, k)$ 
2: for  $o = 1$  to  $O$  do
3:    $(x, y) \leftarrow (\text{RandInt}(0, 100), \text{RandInt}(0, 100))$  ▷ Centroid of trip origin cluster
4:    $\Sigma \leftarrow \text{RandInt}(1, 4) \cdot \begin{pmatrix} 1 & 0 \\ 0 & 1 \end{pmatrix}$  ▷ Covariance matrix of distribution
5:    $\mathcal{O} \leftarrow \mathcal{O} \cup \{\text{Normal}(\begin{pmatrix} x \\ y \end{pmatrix}, \Sigma)\}$  ▷ Two-dimensional pdf of origin cluster
6: for  $d = 1$  to  $D$  do
7:   Execute lines 3-5 on  $\mathcal{D}$  instead of  $\mathcal{O}$  ▷ Trip destination clusters
8:  $F \leftarrow \text{RandomNumberOfTrips}(|\mathcal{N}_c|, T)$ 
9: for  $f = 1$  to  $F$  do
10:   $o \leftarrow \text{RandInt}(1, O)$ ,  $d \leftarrow \text{RandInt}(1, D)$  ▷ Choose indices of origin and destination clusters
11:  Sample  $(x_o, y_o) \sim \mathcal{O}[o]$ ,  $(x_d, y_d) \sim \mathcal{D}[d]$  ▷ Sample start and end locations from pdfs
12:   $(i, j) \leftarrow \text{MapToGrid}((x_o, y_o), (x_d, y_d))$  ▷ Map to nearest discrete grid point
13:   $t \leftarrow \text{SampleStartTime}(1, T)$  ▷ Trip start time
14:   $k \leftarrow \text{CalcTime}((x_o, y_o), (x_d, y_d), v, \Delta t)$  ▷ Trip duration based on SV speed, time discretization
15:   $F_{i,j}^{t,k} \leftarrow F_{i,j}^{t,k} + 1$  ▷ Update nominal demand for tuple  $(i, j, t, k)$ 

```

4.2 Standardized test networks

We generate artificial, standardized test networks on square grids, in order to examine the scaling performance of our algorithm in a systematic manner. For these networks, the SV movement graph $(\mathcal{N}_c, \mathcal{E}_c)$ is fully connected whereas the permitted RV movements, which always take one time step, are determined by Euclidean distance between the stations \mathcal{V}_v and the modelled vehicle speed. We let $\mathcal{N}_v = \mathcal{N}_c$ so that over multiple time steps, RVs can reach and carry out rebalancing actions at all SV nodes.

The clustering of demand at peak times and locations is a primary cause of service degradation for shared mobility systems, and we model it in both the origin and destination of SV journeys. For example, in morning rush hours where SVs are frequently used for the “last mile” of commutes, one encounters high demand for journey starts SVs at incoming commuter rail stations, and high demand for journey ends near workplaces. We use clustering because homogenous demand patterns under-represent the difficulty of typical real-world rebalancing problems. The demand generation procedure is detailed in Algorithm 2.

The algorithm creates a fixed number of Gaussian peaks representing concentrations of trip start locations and trip end locations, and then generates a series of individual “desired trips” for customers. Each desired trip has an origin and destination sampled in continuous 2D space from randomly-indexed origin and destination distributions. The trip’s start time is sampled from a distribution reflecting peaky usage in time, and the duration is inferred from geometry and the SV speed. After running Algorithm 2, one can generate realizations of customer demand by sampling for each tuple (i, j, t, k) from a Poisson distribution with the nominal demand $F_{i,j}^{t,k}$ as the parameter.

4.3 Numerical results

We used a decision horizon of $T = 12$ in all case studies. All journey values were assumed to be distributed uniformly between \$0.50 and \$1.50, regardless of origin, destination, or trip duration. RV movement costs were set to $c_{i,j}^{t,k} = 10^{-3}$ for $i \neq j$ and 0 for $i = j$; load/unload costs were set to 10^{-3} . These penalties were set to very small values purely to discourage arbitrary uncosted RV actions under the initial condition $\bar{V}(y; 0) = 0$, and the main performance metric of interest was the social cost of unserved customer demand.

In Table 6 we report results for the following solution approaches. In each case, the (y, z) decisions from the first stage were made as described, and the objective (2a) was estimated using a Monte Carlo simulation of the second stage cost via (3), averaging over 100 samples for customer demand.

- NA. No action to control the system (no RV movements and $y = 0$).
- M1. SPAR, solving (1) for y and z under the assumption that in the second stage is deterministic, with customer demand $f_{i,j}^{t,k}$ and customer journey values $l_{i,j}^{t,k}(\cdot)$ set to expected values ($F_{i,j}^{t,k}$ rounded to the nearest integer and $l_{i,j}^{t,k}(x) = \frac{1}{2}(l_{\min} + l_{\max})x$ respectively).
- M2-R. SPAR as described in Algorithm 1, but using convex relaxation of problem (7), i.e., non-integral RV routing. After n_{\max} iterations the non-relaxed version of (7) was solved to obtain a feasible solution.
- M2-HI. SPAR as described in Algorithm 1, but with integrality constraints on $z_{i,j}^t$ relaxed for $t > T/2$. As with M3-R, a non-relaxed version of Stage 1 was solved after the n_{\max} “half-relaxed” iterations were completed.
- M2-I. SPAR as described in Algorithm 1, respecting integrality constraints throughout the algorithm.
- M3. SPAR but picking y at random instead of solving problem (7) on line 4. For each tuple (i, t) , the load/unload action was chosen with equal probability from $\{-\bar{y}, -\bar{y} + 1, \dots, \bar{y}\}$. After n_{\max} iterations, solve the first-stage problem (7) to obtain a final output.

We avoided any tuning of the basic algorithm, and used the step size rule suggested in [18], namely $\alpha(n) = 20/(40 + n)$. The anecdotal evidence reported in [18, Figs. 1 (a), (b)] suggests that SPAR may take on the order of only a few tens of iterations to approach a high-quality solution, which is faster than would be explained by the rate of decay of the step size $\alpha(n)$. In our simulations we had a similar experience despite solving a very different problem. We set $n_{\max} = 50$ in all cases, except for M3, where we used 200 iterations to obtain acceptable performance. The latter choice was made as M3 does not benefit from the simultaneous optimization and value function approximation effect observed in the other methods.

For a given size $|\mathcal{N}_c|$, 10 random instances of the artificial networks described in Section 4.2 were created. For each network, the parameters $\bar{d}_i = 10$, $\bar{b} = 5$, $\bar{y} = 10$, $d_i^0 = \bar{d}_i/2$, $\bar{b}_i = 0$ were used. The soft feasibility penalty coefficients described in Section 2.6.1 were set to \$20. RVs were initialized on uniformly random nodes, and only moved fast enough to traverse to an adjacent node (excluding diagonals) in one time step. It was assumed that no SVs were in transit at $t = 0$, and the largest trip duration modelled was $K = 2$ time steps. Fig. 4 shows an example of the VF approximators returned by the algorithm. Fig. 5 shows a representative example of the convergence of the mean service rate, as estimated by the stochastic approximation algorithm. Tables 2 and 3 compares the solution quality in terms of service rate and solution cost, respectively. Table

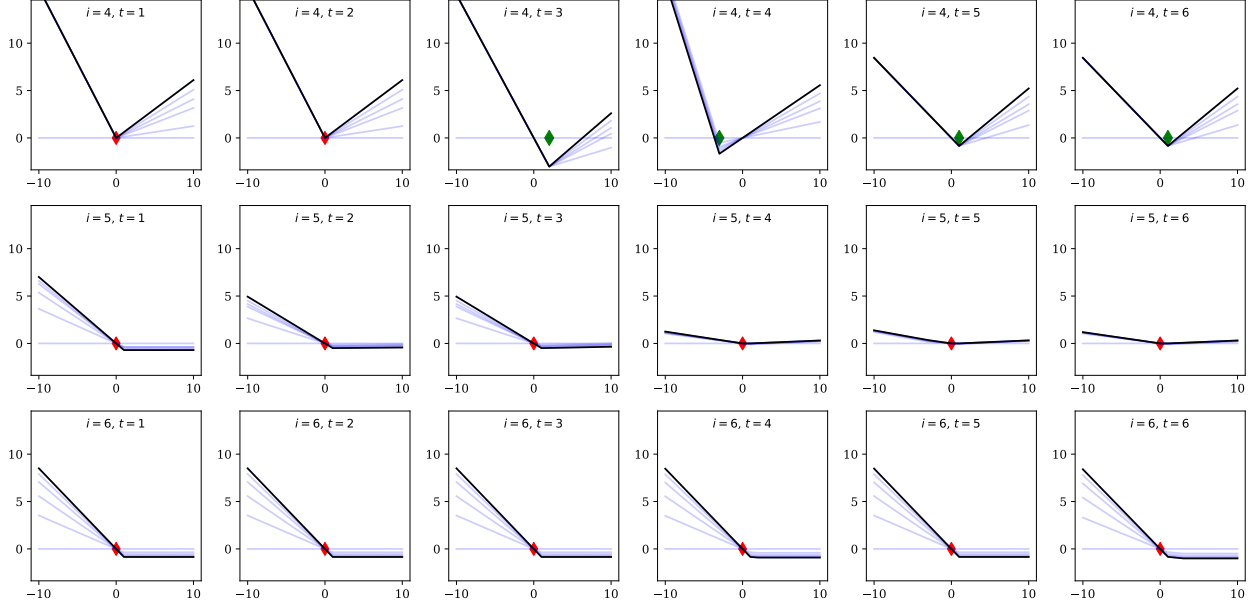


Figure 4: Example of value function approximations $\bar{V}_i^t(y_i^{-,t} - y_i^{+,t})$, for $|\mathcal{N}_c| = 9$ and $|\mathcal{V}| = 1$, for time steps $t = 1$ to 6 at stations 4, 5, and 6. Each plot shows a different (i, t) pair, with the black line showing the final estimate after 50 iterations, and lighter lines showing previous iterations. Markers on the horizontal axis denote load/unload decisions $y_i^{-,t} - y_i^{+,t}$ in the final solution to (7); red indicates no action.

4 reports average time to solve the Stage 1 problem (7) to an MIP tolerance of 5×10^{-3} within M1 and M2 (Stage 1 is not solved in M3). Solution times for Stage 2 are shown in the last column of the table. The hardware used was an Intel Core i7 2.6 GHz CPU, and 16 GB RAM. All problems were solved in Gurobi 7.0.2, with computation confined to 2 CPU threads. Table 5 lists the number of variables and constraints in the first stage problem (7) for method M2-I; some or all integer variables were relaxed in M2-HI and M2-R.

The integer-feasible solutions generated after running each method cause improvements to service rate (or almost equivalently in this setting, solution cost in dollars), for every method, on average – except where only one RV was used on the largest networks. For each solution approach there is also a clear improvement to service rate as the number of RVs increases for a given network size. However some perform better than others. As Table 6 reports, M2-R overstates the flexibility of the RVs by allowing non-integer valued RV flows, effectively allowing them to be in several places at once. Thus, the service rates estimated during the SPAR iterations are over-optimistic, and the final integer solution generated based on the value function approximation obtained is in fact worse than M2-I (see Table 7 and Fig. 5). However, the use of convex relaxations in M2-R dramatically reduces computation time per iteration (see Table 4).

In M2-HI, relaxing the integrality constraints in the second half of the time horizon brings about similar or even better improvements to service rate compared to the full integer solutions in M2-I, and saves roughly one third of computation time. As this application of the SPAR algorithm goes beyond settings where convergence proofs exist, it is not obvious that one should expect M2-R, M2-HI, and M2-I to deliver improving solution quality in that order, and our findings suggest that it is not always better to enforce all first-stage integrality constraints when estimating the second-stage value function. It may be that doing so causes some kind of

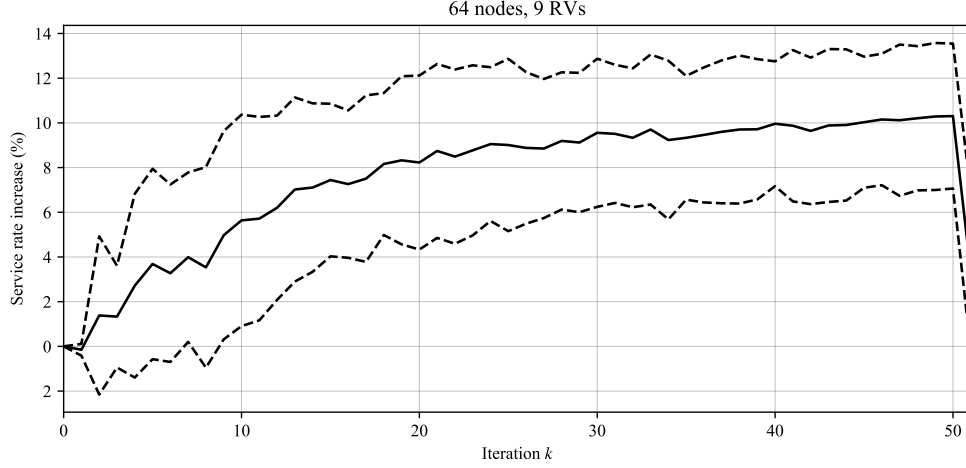


Figure 5: Improvement in modelled service rate in M2-R for $|\mathcal{N}_c| = 64$, $|\mathcal{V}| = 9$. The “51st” iteration is the final integer solution corresponding to the final column of Table 6. Although the mean service rate converges to an improved value, M2-R overstates the flexibility of the RVs during the SPAR iterations, and the final integer solution achieves a lower service rate – in fact, worse than M2-I.

Table 2: Comparison of average service rate in final (integer) solutions, for 10 random systems per row.

$ \mathcal{N}_c $	$ \mathcal{V} $	Svc. rate (%)	Increase in service rate (percentage points); mean \pm standard deviation				
		NA No action	M1 Determin.	M2-R SPAR Relaxed	M2-HI SPAR Half Int.	M2-I SPAR Int.	M3 SPAR Rand.
9	1	80.18 \pm 6.85	6.82 \pm 2.94	4.98 \pm 3.96	7.18 \pm 2.51	7.03 \pm 4.50	1.37 \pm 2.82
	3	80.12 \pm 6.82	9.08 \pm 3.99	4.82 \pm 4.17	7.86 \pm 4.15	6.64 \pm 5.65	4.42 \pm 3.95
16	1	77.94 \pm 2.94	4.69 \pm 1.48	3.23 \pm 1.71	4.85 \pm 2.22	4.68 \pm 2.45	0.71 \pm 0.94
	5	77.69 \pm 2.89	8.80 \pm 1.65	6.43 \pm 3.19	7.83 \pm 1.83	8.00 \pm 1.51	7.23 \pm 3.31
25	1	73.93 \pm 4.85	3.27 \pm 1.56	2.37 \pm 1.93	2.53 \pm 1.41	2.61 \pm 2.00	0.32 \pm 0.76
	5	73.90 \pm 4.90	10.24 \pm 3.27	6.80 \pm 2.37	9.13 \pm 3.73	9.05 \pm 4.27	6.41 \pm 2.44
	9	73.93 \pm 4.83	11.58 \pm 3.95	7.54 \pm 3.38	9.54 \pm 3.30	9.94 \pm 3.75	9.37 \pm 3.52
36	1	73.97 \pm 3.06	2.45 \pm 1.15	1.43 \pm 1.26	1.92 \pm 1.32	1.87 \pm 1.12	0.06 \pm 0.51
	5	74.05 \pm 3.19	8.03 \pm 2.04	6.27 \pm 2.12	8.14 \pm 2.23	6.38 \pm 1.60	5.39 \pm 2.06
	11	73.99 \pm 3.04	9.81 \pm 2.45	6.65 \pm 1.89	10.23 \pm 2.48	8.32 \pm 1.71	6.05 \pm 1.95
64	1	72.40 \pm 3.98	1.11 \pm 0.62	0.11 \pm 0.54	0.36 \pm 0.50	0.88 \pm 0.47	0.02 \pm 0.20
	9	72.60 \pm 4.10	7.49 \pm 2.22	6.81 \pm 2.16	7.91 \pm 1.98	7.37 \pm 2.47	4.65 \pm 2.31
	15	72.43 \pm 4.01	8.72 \pm 2.37	8.12 \pm 2.85	9.61 \pm 2.68	8.07 \pm 2.53	6.17 \pm 1.91
100	1	73.69 \pm 1.95	0.46 \pm 0.50	-0.03 \pm 0.18	0.04 \pm 0.32	0.16 \pm 0.31	-0.04 \pm 0.22
	9	73.67 \pm 1.96	4.90 \pm 0.45	3.95 \pm 1.19	5.31 \pm 0.46	4.83 \pm 0.77	0.72 \pm 0.74
	19	73.67 \pm 2.00	7.10 \pm 1.25	6.14 \pm 1.21	7.83 \pm 1.29	6.72 \pm 1.22	4.46 \pm 1.23
225	1	72.47 \pm 2.37	-0.01 \pm 0.23	-0.00 \pm 0.17	-0.05 \pm 0.15	-0.09 \pm 0.16	0.01 \pm 0.24
	13	72.45 \pm 2.43	3.80 \pm 0.62	2.69 \pm 1.23	3.35 \pm 0.80	3.18 \pm 0.85	0.14 \pm 0.43
	25	72.50 \pm 2.45	5.55 \pm 0.92	4.81 \pm 0.94	5.41 \pm 1.05	4.93 \pm 0.76	2.51 \pm 0.94

Table 3: Comparison of solution cost in final (integer) solution, for 10 random systems per row.

		Sol'n cost (\$)	Absolute change in cost (\$); mean \pm standard deviation				
$ \mathcal{N}_c $	$ \mathcal{V} $	NA	M1	M2-R	M2-HI	M2-I	M3
		No action	Determ.	SPAR Relaxed	SPAR Half Int.	SPAR Int.	SPAR Rand.
9	1	13.16 \pm 5.35	-5.04 \pm 2.26	-3.91 \pm 3.06	-5.41 \pm 2.17	-4.82 \pm 3.20	-1.25 \pm 2.23
	3	13.27 \pm 5.31	-6.27 \pm 2.98	-3.64 \pm 3.24	-5.60 \pm 3.21	-4.85 \pm 4.44	-2.96 \pm 2.95
16	1	28.91 \pm 6.42	-6.80 \pm 2.40	-4.81 \pm 3.17	-7.16 \pm 3.38	-6.97 \pm 4.01	-1.23 \pm 1.67
	5	29.28 \pm 6.08	-12.53 \pm 3.67	-9.31 \pm 4.97	-11.13 \pm 2.74	-11.01 \pm 3.60	-9.93 \pm 5.21
25	1	52.91 \pm 11.92	-7.39 \pm 2.93	-4.88 \pm 4.50	-5.42 \pm 3.23	-5.77 \pm 2.68	-0.27 \pm 1.55
	5	53.18 \pm 12.74	-22.49 \pm 7.86	-15.64 \pm 6.92	-20.09 \pm 8.55	-21.08 \pm 11.00	-14.09 \pm 5.90
	9	53.27 \pm 12.18	-25.22 \pm 9.65	-17.36 \pm 8.64	-21.12 \pm 6.50	-21.70 \pm 8.56	-20.45 \pm 7.71
36	1	73.05 \pm 14.33	-7.49 \pm 3.21	-4.19 \pm 4.27	-6.03 \pm 3.82	-6.39 \pm 3.41	-0.56 \pm 1.73
	5	72.80 \pm 15.01	-24.99 \pm 7.97	-19.56 \pm 6.62	-24.83 \pm 7.48	-19.52 \pm 6.21	-16.95 \pm 7.37
	11	72.97 \pm 14.51	-29.80 \pm 9.92	-20.78 \pm 6.75	-31.20 \pm 8.49	-25.66 \pm 6.16	-17.97 \pm 7.30
64	1	141.61 \pm 34.72	-6.01 \pm 3.78	-0.98 \pm 3.29	-1.53 \pm 3.43	-5.76 \pm 2.59	-0.83 \pm 1.31
	9	139.59 \pm 34.07	-41.76 \pm 14.17	-38.55 \pm 13.76	-43.65 \pm 10.63	-42.51 \pm 14.64	-26.42 \pm 15.79
	15	141.13 \pm 34.62	-47.45 \pm 13.64	-47.10 \pm 20.95	-53.42 \pm 15.87	-43.89 \pm 15.43	-33.89 \pm 13.70
100	1	199.80 \pm 25.40	-3.99 \pm 3.94	0.86 \pm 1.57	-0.14 \pm 3.20	-1.66 \pm 4.14	0.29 \pm 1.60
	9	200.55 \pm 25.51	-40.44 \pm 6.31	-34.58 \pm 11.42	-44.86 \pm 4.85	-40.99 \pm 5.73	-6.86 \pm 7.75
	19	200.63 \pm 26.06	-58.74 \pm 11.10	-52.35 \pm 12.92	-65.47 \pm 12.72	-56.50 \pm 10.68	-37.79 \pm 12.79
225	1	457.94 \pm 78.91	-0.19 \pm 5.00	-0.81 \pm 3.81	0.52 \pm 2.87	1.19 \pm 3.91	-0.94 \pm 5.05
	13	457.91 \pm 78.59	-71.34 \pm 17.27	-52.62 \pm 25.18	-61.70 \pm 18.00	-61.55 \pm 20.09	-2.28 \pm 7.96
	25	457.12 \pm 79.86	-101.34 \pm 24.82	-89.83 \pm 23.30	-100.28 \pm 27.08	-90.53 \pm 19.27	-46.15 \pm 19.25

overfitting of the first-stage solutions.

Method M1 achieves computational times similar to M2-I and worse than M2-HI, and the solution quality is similar to M2-HI. One potential explanation for this is that the stochastic “gradient steps” employed in M2 are rather variable when sampled from the assumed Poisson distribution of customer demand and uniform distribution of trip value. This may lead M1 to make more consistent updates to the approximate value function.

Thanks to the relatively tight relaxation properties of our formulation, we find that in M1 and M2, the solver is able to generate good integer-feasible solutions to these large problems in a short enough time for real-world operational use, meaning substantially less than 1 hour. Further changes to solver parameters, solution tolerances, and the relaxation of different subsets of the integrality constraints could yet improve the trade-off between computation time and solution quality.

The randomness employed in M3 appears to lead to worthwhile improvements in service rate without the costly effort of optimizing the first stage at all during the SPAR iterations. Although more iterations were needed to generate reliable improvements in solution quality, the encouraging results suggest that for even larger systems, meaning $|\mathcal{N}_c|$ of the order several hundred, some kind of random sampling is the only way to manage the scale of the problem. This is because the first-stage problem may become too large to solve fast enough for a real-time rebalancing setting. However, very small systems aside, the solution quality obtained was still somewhat worse than the other methods.

Table 4: Average computation time in seconds per algorithm iteration for M1 and M2. Note Stage 1 is not solved in M3, except for the purpose of generating a final integer-feasible solution at the end. Stage 2 computation times for methods other than M2-I were similar, and are omitted for brevity.

$ \mathcal{N}_c $	$ \mathcal{V} $	Stage 1 (line 4 of Algorithm 1)				Stage 2
		M1	M2-R	M2-HI	M2-I	M2-I
		Determ.	SPAR Relaxed	SPAR Half Int.	SPAR Int.	
9	1	0.135	0.023	0.097	0.127	0.00155
	3	0.224	0.032	0.230	0.457	0.00154
16	1	0.906	0.046	0.215	0.294	0.00228
	5	1.370	0.079	0.734	1.986	0.00231
25	1	1.929	0.081	0.331	0.469	0.00407
	5	3.624	0.145	1.890	3.823	0.00393
	9	1.654	0.167	2.119	6.172	0.00392
36	1	1.207	0.139	0.419	0.587	0.00543
	5	4.121	0.336	2.160	4.363	0.00538
	11	4.569	0.338	5.233	10.780	0.00538
64	1	1.275	0.270	0.678	0.703	0.00951
	9	15.064	0.879	7.585	14.710	0.00912
	15	14.234	0.868	12.371	28.281	0.00953
100	1	1.819	0.563	1.662	1.365	0.01407
	9	27.053	1.448	11.446	17.399	0.01413
	19	29.242	1.963	24.591	44.096	0.01388
225	1	7.389	1.728	5.078	4.871	0.05446
	13	117.257	4.490	28.669	41.649	0.05341
	25	176.919	5.886	64.274	96.225	0.05060

Table 5: Number of variables and constraints in first-stage problem (7) for method M2-I. The numbers of integer and continuous variables are equal in each case, and independent of $|\mathcal{V}|$ owing to the flow formulation.

$ \mathcal{N}_c $	Integer variables	Continuous variables	Constraints
9	1188	1188	3456
16	3456	3456	7488
25	8100	8100	14,400
36	16,416	16,416	25,488
64	50,688	50,688	66,816
100	122,400	122,400	147,600
225	612,900	612,900	669,600

Table 6: Service rate from method M2-R over iterations k . After iteration 50 using a relaxed Stage 1 model, a final integer solution is generated (in contrast to M2-I, Table 7, where iteration 50 generates an implementable integer solution). Values reported as mean \pm standard deviation.

$ \mathcal{N}_c $	$ \mathcal{V} $	Svc. rate (%)	Increase in service rate (percentage points)			
		No action	$k = 10$	$k = 20$	$k = 50$	Final integer
9	1	80.18 \pm 6.85	5.25 \pm 5.40	6.55 \pm 7.29	8.43 \pm 5.78	4.98 \pm 3.96
	3	80.12 \pm 6.82	3.06 \pm 5.24	6.68 \pm 6.10	8.94 \pm 4.47	4.82 \pm 4.17
16	1	77.94 \pm 2.94	5.08 \pm 3.27	5.99 \pm 1.97	6.20 \pm 2.59	3.23 \pm 1.71
	5	77.69 \pm 2.89	-1.67 \pm 3.46	6.55 \pm 2.63	10.10 \pm 2.78	6.43 \pm 3.19
25	1	73.93 \pm 4.85	4.21 \pm 2.90	6.10 \pm 2.16	6.41 \pm 2.26	2.37 \pm 1.93
	5	73.90 \pm 4.90	5.93 \pm 5.18	9.89 \pm 4.22	12.02 \pm 3.69	6.80 \pm 2.37
	9	73.93 \pm 4.83	2.91 \pm 3.28	8.93 \pm 3.74	12.33 \pm 4.38	7.54 \pm 3.38
36	1	73.97 \pm 3.06	3.52 \pm 1.68	3.99 \pm 1.17	4.60 \pm 1.34	1.43 \pm 1.26
	5	74.05 \pm 3.19	5.52 \pm 3.10	8.11 \pm 3.21	10.31 \pm 2.84	6.27 \pm 2.12
	11	73.99 \pm 3.04	0.42 \pm 2.98	9.71 \pm 2.64	11.46 \pm 2.04	6.65 \pm 1.89
64	1	72.40 \pm 3.98	1.90 \pm 1.19	2.54 \pm 0.93	2.24 \pm 0.59	0.11 \pm 0.54
	9	72.60 \pm 4.10	5.75 \pm 3.40	9.34 \pm 2.74	10.96 \pm 2.59	6.81 \pm 2.16
	15	72.43 \pm 4.01	3.12 \pm 4.90	9.38 \pm 3.75	12.75 \pm 3.38	8.12 \pm 2.85
100	1	73.69 \pm 1.95	1.29 \pm 0.33	1.43 \pm 0.40	1.56 \pm 0.33	-0.03 \pm 0.18
	9	73.67 \pm 1.96	4.08 \pm 1.32	6.24 \pm 0.97	8.15 \pm 0.72	3.95 \pm 1.19
	19	73.67 \pm 2.00	1.99 \pm 1.63	8.21 \pm 1.40	10.40 \pm 1.53	6.14 \pm 1.21
200	1	72.47 \pm 2.37	0.53 \pm 0.34	0.53 \pm 0.18	0.71 \pm 0.17	-0.00 \pm 0.17
	13	72.45 \pm 2.43	3.35 \pm 1.23	4.78 \pm 1.03	5.89 \pm 0.75	2.69 \pm 1.23
	25	72.50 \pm 2.45	3.65 \pm 1.31	6.57 \pm 1.16	8.58 \pm 1.03	4.81 \pm 0.94

Table 7: Improvement in service rate from method M2-I over iterations k . Values reported as mean \pm standard deviation. The “No action” column reports the baseline service rate, and differ slightly between rows for a given $|\mathcal{N}_c|$ due to independent sampling of customer demand. The statistics reported in each row are for 10 independent test networks. Values reported as mean \pm standard deviation.

$ \mathcal{N}_c $	$ \mathcal{V} $	Svc. rate (%)	Increase in service rate (percentage points)		
		No action	$k = 10$	$k = 20$	$k = 50$
9	1	79.96 \pm 7.10	5.96 \pm 4.27	6.07 \pm 5.15	7.03 \pm 4.50
	3	80.51 \pm 6.86	4.47 \pm 6.17	6.18 \pm 4.70	6.64 \pm 5.65
16	1	77.54 \pm 3.16	3.84 \pm 2.34	3.69 \pm 1.84	4.68 \pm 2.45
	5	77.81 \pm 3.02	4.76 \pm 2.30	5.99 \pm 2.88	8.00 \pm 1.51
25	1	74.03 \pm 4.81	1.90 \pm 2.16	2.27 \pm 1.87	2.61 \pm 2.00
	5	74.03 \pm 5.03	7.17 \pm 4.68	8.23 \pm 4.28	9.05 \pm 4.27
	9	73.89 \pm 4.85	7.35 \pm 6.01	7.66 \pm 4.33	9.94 \pm 3.75
36	1	74.11 \pm 3.04	1.24 \pm 0.67	1.51 \pm 0.82	1.87 \pm 1.12
	5	74.01 \pm 2.94	4.37 \pm 2.15	5.45 \pm 1.13	6.38 \pm 1.60
	11	74.18 \pm 3.01	5.22 \pm 2.17	6.19 \pm 2.38	8.32 \pm 1.71
64	1	72.47 \pm 4.15	0.75 \pm 0.52	0.72 \pm 0.64	0.88 \pm 0.47
	9	72.47 \pm 4.03	5.37 \pm 2.25	6.44 \pm 2.23	7.37 \pm 2.47
	15	72.44 \pm 3.98	6.12 \pm 2.44	6.81 \pm 2.50	8.07 \pm 2.53
100	1	73.74 \pm 1.95	0.13 \pm 0.34	0.13 \pm 0.42	0.16 \pm 0.31
	9	73.63 \pm 1.95	3.63 \pm 0.49	4.10 \pm 0.55	4.83 \pm 0.77
	19	73.72 \pm 1.97	4.72 \pm 1.42	5.82 \pm 1.13	6.72 \pm 1.22
225	1	72.53 \pm 2.37	0.10 \pm 0.16	-0.07 \pm 0.20	-0.09 \pm 0.16
	13	72.54 \pm 2.39	2.58 \pm 0.91	2.81 \pm 0.89	3.18 \pm 0.85
	25	72.47 \pm 2.38	3.61 \pm 0.76	4.15 \pm 0.53	4.93 \pm 0.76

Table 8: Solution statistics and computation time for the Philadelphia case study (mean \pm std. dev.).

	M1	M2-R	M2-HI	M2-I	M3
Service rate change (%)	2.290 \pm 0.590	3.742 \pm 0.877	4.538 \pm 0.810	3.013 \pm 1.295	3.597 \pm 1.485
Cost change (\$)	-11.23 \pm 3.19	-18.20 \pm 4.04	-20.96 \pm 4.05	-12.21 \pm 6.17	-14.03 \pm 6.24
Stage 1 time (s)	138.0 \pm 228.3	3.504 \pm 1.173	16.61 \pm 30.69	14.06 \pm 58.24	— [†]
Stage 2 time ($\times 10^{-3}$ s)	15.73 \pm 5.62	21.32 \pm 6.91	22.04 \pm 7.10	21.38 \pm 6.87	19.31 \pm 4.73
Final integer solution time* (s)	— [†]	456.7 \pm 410.3	152.7 \pm 158.9	— [†]	1200 \pm 0

* Timeout set to 1200 s. Solution stats reported are for best solution available at timeout.

[†] Not required in this method.

4.4 Philadelphia case study

Experiments were run on a model of the Philadelphia bike sharing system, with $|\mathcal{N}_c| = 102$ docking stations and 1103 bikes, parameterized using public customer journey data from April 2015 to June 2017. The methods described above were applied to a 3-hour time horizon containing $T = 12$ steps of 15 minutes starting at 8am, with the customer demand data $F_{i,j}^{t,k}$ corresponding to rates measured for a June weekday. The maximum journey duration modelled was $K = 4$ time steps, i.e., 1 hour. We assumed $|\mathcal{V}| = 15$ RVs (i.e., repositioning trucks) were present, each with capacity $\bar{d} = 10$. The speed of the RVs travelling around the city was such that on average 16% of stations were reachable in one time step from any other station. The parameterization of the methods was otherwise the same as in Section 4.3. We performed 10 tests of the methods, corresponding to 10 different random initial locations of the RVs.

The average service rate under no rebalancing actions was 69.96%, and the average customer demand was approximately 450 trips during the planning horizon. Results in terms of service rate, cost, and computation time are shown in Table 8. Method M1 performed the worst, caused by the limitation of the deterministic, integer-valued representation of second-stage demand. For this system the average demand $F_{i,j}^{t,k}$ per 15 minute interval was below 0.5 for most tuples (i, j, t, k) , and these were rounded down to 0, meaning the RVs were scheduled against an underestimate of customer demand. Agreeing with or magnifying the findings in Section 4.3, the results using the relaxations in M2-R and M2-HI were superior to those using full integer solutions in M2-I. Methods M2-R and M3 yielded good results, although the final integer solution was much slower to generate, often timing out at the pre-set limit of 1200 seconds. In cases where a timeout did occur, the suboptimality bound was between 1% and 2%.

5 Conclusion

We described and validated a scalable approach to look-ahead optimization of shared mobility systems in real time, intended for a system operator wishing to maximize service rate by redistributing SVs in parallel with customers using the system. The method is able to handle stochastic customer demand patterns without resorting to queueing or inventory models and their associated limitations. The method offers the flexibility needed for a time-constrained implementation, in that the SPAR iterations can be limited in number, or accelerated by using linear relaxations. In variants M2-R, M2-HI, and M3, where a final integer solution needs to be computed after the SPAR iterations, this computation can also be terminated early if required,

as feasible approximate solutions to (7) are trivial for the solver to find. Lastly, the approximate value functions $\bar{V}_i^t(\cdot)$ are useful as an operational indicator of SV surplus or shortfall, and could perhaps be used as an input to other, non-solver-based heuristics for making rebalancing decisions.

The approach we have presented is intended to be used as part of a real-time scheme in which the system operator plans several hours ahead with the aid of a stochastic demand model. After a short time has elapsed, corresponding to one or more discrete time steps modelled, a new optimization would be carried out in light of the new state measurement and updated demand forecast. This “receding horizon” control scheme would resemble model predictive control (MPC) [6]. An important consideration in MPC is the penalty function assigned to the system state at the end of the optimization horizon; this “terminal cost” should reflect the value function (in the dynamic programming sense) of an underlying problem over a much longer planning horizon. It may be possible to use the same separable function approximation approach as we used here to derive suitable terminal costs for this problem.

A future direction with real-world implications is to consider the limit to station-free, also known as free-floating, mobility systems, in which the number of nodes conceptually tends to infinity and uncertainties are described by continuous probability distributions. In this setting one must find an alternative way to map the infinite-dimensional input data to a finite decision problem at acceptable computational cost, identifying a suitable basis for the value function approximation in the process.

Acknowledgments

J. Warrington gratefully acknowledges a visiting fellowship funded by the Simons Institute for the Theory of Computing at UC Berkeley, USA, for the Spring Semester of 2018. Most of the work for this study was carried out there. He also thanks Jannik Matuschke of Technische Universität München, Germany, for informative conversations on network flow problems, and both authors thank Lioba Heimbach and Christoph Adam at ETH Zurich for data processing efforts in an earlier project related to the Philadelphia case study.

References

- [1] Ravindra K. Ahuja, Thomas L. Magnanti, and James B. Orlin. Network flows. 1988.
- [2] Javier Alonso-Mora, Samitha Samaranyake, Alex Wallar, Emilio Frazzoli, and Daniela Rus. On-demand high-capacity ride-sharing via dynamic trip-vehicle assignment. *Proceedings of the National Academy of Sciences*, 114(3):462–467, January 2017.
- [3] Siddhartha Banerjee, Ramesh Johari, and Carlos Riquelme. Pricing in Ride-Sharing Platforms: A Queueing-Theoretic Approach. In *Proceedings of the Sixteenth ACM Conference on Economics and Computation*, EC ’15, pages 639–639, New York, NY, USA, 2015. ACM.
- [4] Siddhartha Banerjee, Yash Kanoria, and Pengyu Qian. The Value of State Dependent Control in Ridesharing Systems. *arXiv:1803.04959 [math]*, March 2018. arXiv: 1803.04959.
- [5] V.S. Borkar. *Stochastic Approximation: A Dynamical Systems Viewpoint*. Springer, 2009.

- [6] Francesco Borrelli, Alberto Bemporad, and Manfred Morari. *Predictive Control for Linear and Hybrid Systems*. Cambridge University Press, 2017.
- [7] Jan Brinkmann, Marlin W. Ulmer, and Dirk C. Mattfeld. Dynamic Lookahead Policies for Stochastic-Dynamic Inventory Routing in Bike Sharing Systems. *Computers & Operations Research*, June 2018.
- [8] Lucian Busoniu, Robert Babuska, Bart De Schutter, and Damien Ernst. *Reinforcement learning and dynamic programming using function approximators*, volume 39. CRC press, 2010.
- [9] A. V. Fiacco and J. Kyriasis. Convexity and concavity properties of the optimal value function in parametric nonlinear programming. *Journal of Optimization Theory and Applications*, 48(1):95–126, January 1986.
- [10] Marshall L. Fisher. An Applications Oriented Guide to Lagrangian Relaxation. *Interfaces*, 15(2):10–21, April 1985.
- [11] Supriyo Ghosh, Pradeep Varakantham, Yossiri Adulyasak, and Patrick Jaillet. Dynamic Repositioning to Reduce Lost Demand in Bike Sharing Systems. *Journal of Artificial Intelligence Research*, 58:387–430, February 2017.
- [12] Benjamin Legros. Dynamic repositioning strategy in a bike-sharing system; how to prioritize and how to rebalance a bike station. *European Journal of Operational Research*, July 2018.
- [13] Neda Masoud and R. Jayakrishnan. A real-time algorithm to solve the peer-to-peer ride-matching problem in a flexible ridesharing system. *Transportation Research Part B: Methodological*, 106:218–236, December 2017.
- [14] Rahul Nair and Elise Miller-Hooks. Fleet Management for Vehicle Sharing Operations. *Transportation Science*, 45(4):524–540, 2011.
- [15] Aritra Pal and Yu Zhang. Free-floating bike sharing: Solving real-life large-scale static rebalancing problems. *Transportation Research Part C: Emerging Technologies*, 80:92–116, July 2017.
- [16] M. V. F. Pereira and L. M. V. G. Pinto. Multi-stage stochastic optimization applied to energy planning. *Mathematical Programming*, 52(1-3):359–375, May 1991.
- [17] J. Pfrommer, J. Warrington, G. Schildbach, and M. Morari. Dynamic vehicle redistribution and online price incentives in shared mobility systems. *IEEE Transactions on Intelligent Transportation Systems*, 15(4):1567–1578, 2014.
- [18] Warren Powell, Andrzej Ruszczycki, and Huseyin Topaloglu. Learning Algorithms for Separable Approximations of Discrete Stochastic Optimization Problems. *Mathematics of Operations Research*, 29(4):814–836, November 2004.
- [19] Warren B. Powell and Huseyin Topaloglu. Stochastic Programming in Transportation and Logistics. In *Handbooks in Operations Research and Management Science*, volume 10 of *Stochastic Programming*, pages 555–635. Elsevier, January 2003.
- [20] Tal Raviv and Ofer Kolka. Optimal inventory management of a bike-sharing station. *IIE Transactions*, 45(10):1077–1093, 2013.

- [21] Tal Raviv, Michal Tzur, and Iris A. Forma. Static repositioning in a bike-sharing system: models and solution approaches. *EURO Journal on Transportation and Logistics*, pages 1–43, 2013.
- [22] Robert Regue and Will Recker. Proactive vehicle routing with inferred demand to solve the bikesharing rebalancing problem. *Transportation Research Part E: Logistics and Transportation Review*, 72:192–209, December 2014.
- [23] Mauro Salazar, Federico Rossi, Maximilian Schiffer, Christopher H. Onder, and Marco Pavone. On the Interaction between Autonomous Mobility-on-Demand and Public Transportation Systems. *arXiv:1804.11278 [cs]*, April 2018. arXiv: 1804.11278.
- [24] J. Schuijbroek, R. C. Hampshire, and W. J. van Hoes. Inventory rebalancing and vehicle routing in bike sharing systems. *European Journal of Operational Research*, 257(3):992–1004, March 2017.
- [25] Rick Zhang, Federico Rossi, and Marco Pavone. Routing Autonomous Vehicles in Congested Transportation Networks: Structural Properties and Coordination Algorithms. *Autonomous Robots*, in press, 2018.